J Eng Math (2015) 90:37–49
DOI 10.1007/s10665-014-9726-1

Electromagnetic force on a current-carrying coil interacting with a moving electrically conducting cylinder

F. B. Santara · A. Thess

Received: 12 July 2013 / Accepted: 14 July 2014 / Published online: 1 November 2014

Abstract We present a numerical analysis of a variant of Lorentz force velocimetry (LFV) termed electromagnetic Lorentz force velocimetry (EM–LFV). Both LFV and EM–LFV are techniques for the non-contact measurement of liquid metal flows in metallurgical applications that rely on the measurement of a force acting upon a magnetic system interacting with the liquid metal. Whereas LFV relies on permanent-magnet systems, EM–LFV is based upon electromagnets. We formulate and analyse a simple model of EM–LFV which consists of a single circular coil interacting with a moving solid cylinder. We compute the Lorentz force acting on the coil as a function of the two geometry parameters characterizing the problem and compare the numerical results with analytical approximations for three limiting cases. Our numerical results serve as a verification and validation tool for future full-scale simulations of EM–LFV involving realistic complex electromagnets and three-dimensional turbulent flow geometries.

Keywords Computational magneto-hydrodynamics · Lorentz force velocimetry · Electromagnet

1 Introduction

Velocity measurement techniques constitute a challenging field for the industry of metal manufacturing because of the aggressive environment which accompanies their melting process, which always occurs at high temperatures. Several techniques are detailed in [1]. As can be easily understood, conventional techniques which require contact between the sensors and the liquid are not suitable to measure the velocity of a liquid metal. Therefore, non-contact flow measurement techniques represent a challenging and interesting field with obvious applications. Measurement techniques, including non-contact methods, for liquid metals can be found in the literature, but they remain commercially unavailable. One of the first works in the theory of flow measurement using a magnetic field was established in the early 1960s by Shercliff [2], who developed the theory of the magnetic flywheel, followed by an analysis of flowmeters based on a multi-coil system presented by Feng et al. [3].

More recent works are also available classified under either *flowmeter* [4,5] or *Lorentz force velocimetry* (LFV). The LFV method has been widely investigated during the last decade: physical principles [6,7], numerical simu-

F. B. Santara (✉) · A. Thess
Institute of Thermodynamics and Fluid Mechanics, Ilmenau University of Technology,
P.O. Box 100565, 98684 Ilmenau, Germany
e-mail: fatoumata.bintou.santara@gmail.com

lations [8,9], experiments at the laboratory scale [10–12] and validation at the industrial scale [13]. Most of these studies were carried out for cases where a localized magnetic field is created by permanent magnets or a magnetic dipole. This measurement system may be more expensive for wide and complex industrial installations. In particular, attention may be drawn to the work of Kirpo et al. [8] who conducted investigations similar to the one we are performing here, computing the electromagnetic drag force and torque due to the motion of a solid bar, but in the case where the magnetic field is created by a magnetic dipole.

The so-called *electromagnetic Lorentz force velocimetry* (EM–LFV) is proposed here as an alternative; it creates magnetic fields by means of electromagnets. Similar works using coils exist in the literature. For instance Feng et al. investigated and optimized some arrangements of multi-coil flowmeters [3] creating an AC magnetic field. The difference with the LFV method is the use of a coil as a steady magnetic field source instead of a permanent magnet or magnetic dipole.

Our interest in electromagnets as the source of a magnetic field in this study is motivated by the eventuality of an increase in the LFV process cost in large-scale industrial uses. Indeed, the geometries used in the industry cover a scale varying from the centimetre to meter range, and subsequently much greater Lorentz force flowmeter may be required to measure velocity and mass flux under such conditions. The cost of a permanent magnet increases with its size, which leads to higher process costs for the Lorentz force flowmeter. In such a case, the use of an electromagnet consisting of a simple copper coil will ensure a reasonable process cost in industrial-scale applications. In addition, the magnetic field created by an electromagnet can be switched off if needed during the process, which is an advantage over magnet systems.

The present work aims to determine analytically the Lorentz force resulting in the motion of an electrically conducting solid body under a steady magnetic field created by a coil through the coefficient of sensitivity of the flowmeter. This non-dimensional coefficient is a term that appears in the analytical formulation of the Lorentz force as a function of different geometrical parameters: the radius of the inducting coil, the radius of the electrically conducting solid body, and the distance between the coil and the conducting solid body, which are summarized under two dimensionless parametersm C_1 and C_2, whose variations make it possible to investigate all geometries which can be theoretically or practically achieved. The Lorentz force and the coefficient of sensitivity are then computed numerically and compared to the analytical solutions.

This paper is organized as follows. The studied cases and the main geometrical parameters are introduced in Sect. 2. Then the analytical formulation for the Lorentz force and the coefficient of sensitivity are defined in Sect. 3. Section 4 presents the computation results and their comparison with the analysis. Finally, concluding remarks are made in Sect. 5.

2 Methodology

We are interested in a simple geometry (Fig. 1). It consists of an electrically conducting solid body (referred to as a cylinder) and a coil which creates the steady magnetic field when subjected to a steady current. The coil is centred regarding the cylinder and is placed at the position $z = 0$, where z is the axial coordinate. The radius of the cylinder is denoted by R_{cyl}, R_{coil} is the thickness of the coil and R is the curvature radius of the coil.

Two dimensionless geometrical parameters were defined related to that configuration in order to have a complete description of all situations which can theoretically emerge. These parameters are respectively C_1 and C_2, defined as

$$C_1 = \frac{R_{\mathrm{cyl}}}{R} \tag{1}$$

and

$$C_2 = \frac{R_{\mathrm{coil}}}{R}, \tag{2}$$

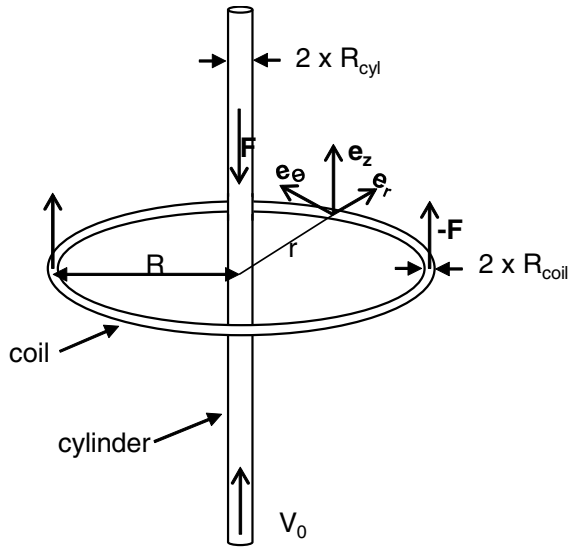

Fig. 1 Geometry of solid body of radius R_{cyl} and coil of radius R_{coil}. R is the curvature radius of the coil

where C_1 is the ratio of the radius of the cylinder to the curvature radius of the coil (1) and C_2 is the ratio of the radius of the coil to the curvature radius of the coil (2).

The aim is to compute the Lorentz force acting upon the coil in the vertical direction (z) as a function of C_1 and C_2 as well as the current I, the conductivity of the coil σ and the radius of the cylinder when the cylinder moves in the z-direction at velocity V_0. A broad range of points of investigation (Fig. 2) was defined based on these dimensionless numbers. As presented in Fig. 1, the radii R_{cyl} and R_{coil} must satisfy the inequality (3):

$$R \geq R_{cyl} + R_{coil}. \tag{3}$$

Using (1) and (2) with (3), this implies

$$C_1 + C_2 \leq 1. \tag{4}$$

These points vary in a range of between 0 and 1 since C_1 and C_2 must satisfy relation (4). This relation is illustrated by the diagonal line drawn in Fig. 2, where it can be easily seen that $C_1 = 0$ corresponds to $C_2 = 1$ and vice versa. For cases where $C_1 + C_2 = 1$ the computation point is localized on the diagonal line. When $C_1 + C_2 < 1$, the computation point is localized under the diagonal line. Therefore, the corresponding values of C_1 and C_2 lead to a set of points which form a triangle having three vertices localized at respectively $C_1 = C_2 = 0$, $C_1 = 1$ and $C_2 = 1$. These points correspond to three asymptotic situations which cannot be reached in practice. Thus, three cases which approach these asymptotic situations were studied and defined as follows: when C_1 and $C_2 \to 0$, the investigated point tends towards the first vertex localized at $(0, 0)$. When $C_1 \to 1$ and $C_2 \to 0$, the studied case tends towards the second vertex at $(1, 0)$. Finally, when $C_1 \to 0$ and $C_2 \to 1$, we approach the third vertex at $(0, 1)$.

Figure 3 shows an illustration of these limiting cases. A situation where the radius of the cylinder R_{cyl} is much smaller compared with the curvature radius of the coil R is shown in Fig. 3a. This case was previously investigated and published in [7].

The second case presented in Fig. 3b corresponds to a situation where the thickness of the coil is infinitesimally small and when it is wrapped around the moving cylinder, leaving no gap. Although this case is far from representing a realistic situation, it is conceptually important because it provides an upper bound on the Lorentz force.

The last situation is illustrated in Fig. 3c: a thick coil is wrapped around an infinitesimally thin cylinder, leaving no gap in order to have R very close to R_{coil}.

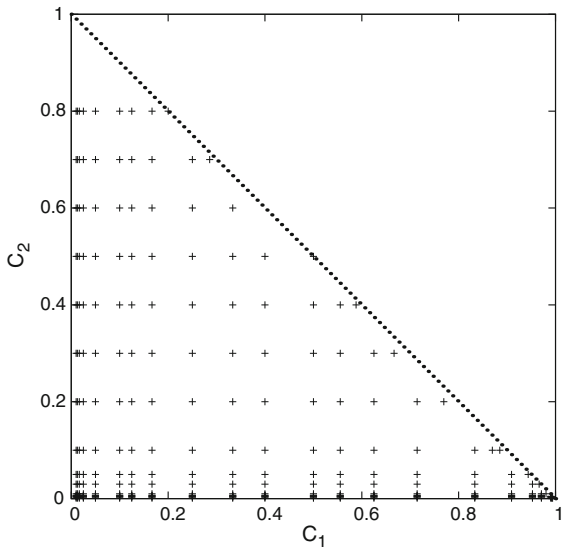

Fig. 2 Investigation domain defined by geometrical parameters C_1 and C_2, which vary in a range of 0 to 1. The *diagonal line* and the *three vertices* define the limits of that domain

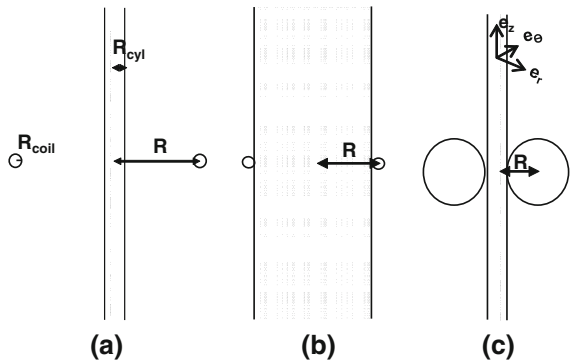

Fig. 3 Sketch of three limiting cases: **a** the radii of both the cylinder and the coil are small compared to R: $R_{\text{cyl}} = \epsilon R$, $R_{\text{coil}} = \epsilon R$ or $C_1 = \epsilon$, $C_2 = \epsilon$; **b** the radius of the coil is much smaller than the radius of the cylinder: $R_{\text{coil}} = \epsilon R_{\text{cyl}}$ or $C_2 = \epsilon$, $\epsilon \ll 1$; **c** the radius of the cylinder is much smaller than the radius of the coil: $R_{\text{cyl}} = \epsilon R_{\text{coil}}$ or $C_1 = \epsilon$, $\epsilon \ll 1$

3 Analytical approximations

Theoretical investigations were made for the kinematic–solid body motion problem (where the velocity is implemented in calculations as a constant) based on the principles of electromagnetism. An analysis of the three limiting cases introduced previously is presented in this section.

3.1 Thin cylinder–thin coil

A geometry consisting of a thin cylinder and a thin coil reflects the condition where both C_1 and C_2 are infinitesimally small (Fig. 3a). Indeed, since $R_{\text{cyl}} = \epsilon R$ and $R_{\text{coil}} = \epsilon R$, it happens, according to Eqs. (1) and (2) respectively, that $C_1 = \epsilon$ and $C_2 = \epsilon$, which also confirm Eq. (4).

The condition $C_1 = \epsilon$ can also be written as $C_1 \ll 1$. Here, we refer to a previous work of Thess et al. [7], where this case was investigated. The analytical solution of the Lorentz force F_1 was formulated in the case of an electrically conducting material (being either a solid body or a melt) moving at a velocity V_0 in a localized region where a steady magnetic field exists. This solution is given by the following relation (derived in [7]):

$$F_1 = -\frac{45\pi^2}{256}\frac{\sigma V_0 B_0^2 R_{\text{cyl}}^4 S_1}{R}. \tag{5}$$

Here, B_0 is the maximum value reached by the magnetic flux density at the centre of the cylinder, σ is the electrical conductivity of the cylinder and V_0 is its moving velocity. Moreover, R_{cyl} and R are respectively the radius of the cylinder and the curvature radius of the coil. The coefficient S_1 is the sensitivity of the flowmeter.

This dimensionless quantity has been defined by Shercliff as a "measure of the performance or the calibration of any induction flowmeter in which the potential difference induced between two electrodes is used to indicate

a flow rate" [2].[1] According to this primary definition, another formulation was established by Thess et al. [7], where the coefficient of sensitivity of the flowmeter is directly related to the non-dimensional shape function of the velocity profile. We refer to that formulation in this paper. Its value depends on the motion type, i.e. a solid body translation or the Poiseuille flow of a liquid. Here, index 1 denotes that the coefficient is related to the Lorentz force termed F_1. This nomenclature is subsequently generalized in this paper. For the conditions $C_1 = \epsilon$ and $C_2 = \epsilon$, combined with a solid body motion under a steady magnetic field, it was established that the coefficient of sensitivity $S_1(C_1, C_2) = S_1$ is a constant equal to 1/4 [7]. The dependency of S_1 on C_1 and C_2 appears once the non-dimensional numbers are no longer negligible.

We reformulate this equation to underscore the dependency of the Lorentz force on the current instead of the magnetic field, replacing B_0 with $\mu_0 I/(2R)$, which leads to

$$F_1 = -\frac{45\pi^2}{256}\frac{\sigma V_0 \mu_0^2 I^2 R_{\text{cyl}}^4 S_1}{4R^3}. \tag{6}$$

where F_1 is the axial component of the Lorentz force. We notice that the radius of the coil does not appear in Eqs. (5) and (6), and then C_2 has no effect on the Lorentz force for a given value of the inductor's current. The Lorentz force increases with R_{cyl} due to its dependency on R_{cyl}^4 and increases when R decreases because the distance to the coil decreases, leading to a higher level of exposition of the cylinder to the magnetic field. The magnitude of that analytical Lorentz force calculated for $R_{\text{cyl}} = 0.001\,\text{m}$, $\sigma = 10^6\,\text{S/m}$, $V_0 = 10\,\text{m/s}$ is typically of $1.71 \times 10^{-12}\,\text{N}$ when $R = 1\,\text{m}$ and $7.93 \times 10^{-12}\,\text{N}$ when $R = 0.6\,\text{m}$. This non-realistic numerical example only illustrates how weak the Lorentz force is for large radii of a coil.

3.2 Thick cylinder–thin coil

This situation is related to that in Fig. 3b, where the radius of the coil is negligible compared with the radius of the cylinder: $R_{\text{coil}} = \epsilon R_{\text{cyl}}$, with $\epsilon \ll 1$.

Therefore,

$$R = R_{\text{cyl}} + R_{\text{coil}} = R_{\text{cyl}}(1 + \epsilon) \tag{7}$$

and

$$C_1 \simeq 1 - \epsilon, \tag{8}$$

$$C_2 \simeq \epsilon. \tag{9}$$

When $\epsilon \ll 1$, R_{cyl} is close to R, which tends towards infinity. Therefore, R_{coil} is so small compared to R_{cyl} that the situation is equivalent to a wire coil creating a magnetic field in a semi-infinite plane (Fig. 4) (the plane is infinite along the axial z-direction and semi-infinite along the radial r-direction). The expression for the Lorentz force F_2 is obtained after a change of reference from a cylindrical coordinate to a Cartesian coordinate system.

Strictly speaking, the magnetic field created in such a configuration has an infinite magnitude when $R = 0$. The subsequent Lorentz force integrated in an infinite plane is infinite itself. However, this extreme approximation is retained, which allows a change in reference from a cylindrical coordinate to a Cartesian coordinate system. The origin is located at the centre of the coil. Thus, the magnetic flux density created by an infinite wire is given by the Biot–Savart law as

$$\vec{B} = \frac{\mu_0 I}{2\pi r}\vec{e_\theta}. \tag{10}$$

[1] This statement is part of the original text.

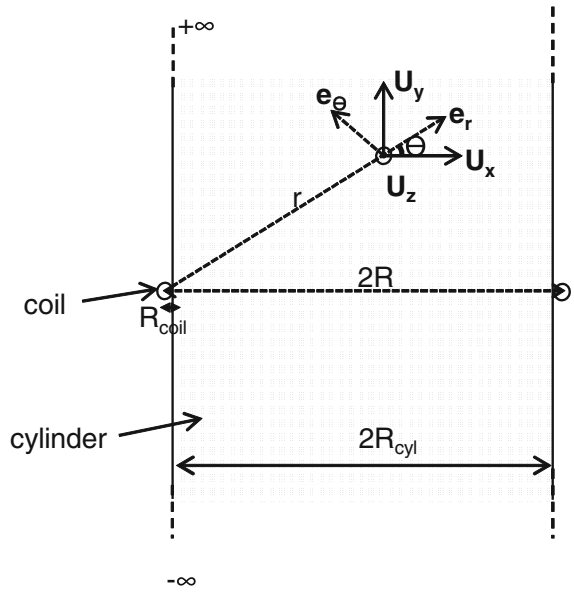

Fig. 4 Infinitely long wire (in z-direction) and semi-infinite plane having an infinite length along axial direction z and a semi-infinite length along radial direction: R_{cyl} is close to R, which is much higher compared with R_{coil}

Since $\vec{e_\theta} = \cos\theta \vec{U}_y - \sin\theta \vec{U}_x$, and knowing that $\cos\theta = x/r$ and $\sin\theta = y/r$, the magnetic flux density is written in Cartesian coordinates as

$$\vec{B} = \frac{\mu_0 I}{2\pi}\frac{x}{r^2}\vec{U}_y - \frac{\mu_0 I}{2\pi}\frac{y}{r^2}\vec{U}_x. \tag{11}$$

The eddy current induced in the volume of our cylinder is

$$\vec{J} = \sigma \vec{V} \times \vec{B}, \tag{12}$$

where $\vec{V} = V_0\vec{U}_y$ is the moving velocity of the coil and $\vec{B} = B_x\vec{U}_x + B_y\vec{U}_y$ is the magnetic field (Eq. 11).

Finally, we obtain

$$\vec{J} = \sigma V_0 \frac{\mu_0 I}{2\pi}\frac{y}{x^2+y^2}\vec{U}_z. \tag{13}$$

Then the Lorentz force can be calculated as

$$\vec{f} = \vec{J} \times \vec{B} = -J_z B_y \vec{U}_x + J_z B_x \vec{U}_y. \tag{14}$$

We are only interested in the y component of the Lorentz force, termed F_2 here. We can now revisit the cylindrical coordinate system to integrate the Lorentz force in the volume of the cylinder. In the cylindrical coordinate system, y remains unchanged and x becomes $R - r$. The y component of the volumetric Lorentz force shown in (14) is then integrated as follows:

$$\begin{aligned} F_2 &= -\sigma V_0 \left(\frac{\mu_0 I}{2\pi}\right)^2 \int_{-\infty}^{\infty}\int_0^{R_{\text{cyl}}} \frac{y^2}{((R-r)^2+y^2)^2} 2\pi r \,\mathrm{d}r\,\mathrm{d}y \\ &= -\sigma V_0 \left(\frac{\mu_0 I}{2}\right)^2 \left[R \ln\left(\frac{R_{\text{cyl}}}{R_{\text{coil}}}+1\right) - R_{\text{cyl}}\right]. \end{aligned} \tag{15}$$

Table 1 Analytical values for non-dimensional coefficient of sensitivity of flowmeter $S_2(C_1, C_2)$ computed as function of non-dimensional parameters C_1 and C_2 (when $C_1 = 1 - \epsilon$ and $C_2 = \epsilon$) and corresponding values for analytical Lorentz force $|F_2|$ (absolute value, unit is N)

C_1	C_2	$S_2(C_1, C_2)$	$\lvert F_2\rvert$
0.99	0.010	4.5952	0.1814
0.992	0.008	4.8183	0.1902
0.996	0.004	5.5115	0.2176
0.997	0.003	5.7991	0.2289
0.998	0.002	6.2046	0.2449

Using the definition of the dimensionless parameters (Eqs. 1 and 2), relation (15) leads to the following formulation:

$$F_2 = -\sigma V_0 \frac{\mu_0^2 I^2}{4} \left[R \ln \left(\frac{C_1}{C_2} + 1 \right) - R_{\text{cyl}} \right]. \tag{16}$$

Note that when we consider an infinite value for C_1, Eq. (16) becomes infinite, which corresponds to the semi-infinite plane situation. In the same way, considering $C_2 = 0$, a similar analysis can be acrried out, and we find the thin wire case.

Defining the coefficient of sensitivity as $S_2(C_1, C_2) = R \ln \left(\frac{C_1}{C_2} + 1 \right) - R_{\text{cyl}}$ (where index 2 denotes the relation to F_2), Eq. (16) becomes

$$F_2 = -\sigma V_0 \frac{\mu_0^2 I^2}{4} S_2(C_1, C_2). \tag{17}$$

Table 1 summarizes the analytical values reached by S_2 and F_2 when $C_2 = \epsilon \ll 1$ and $C_1 = 1 - \epsilon \simeq 1$. An increase of the Lorentz force is observed with C_1 (which varies from 0.99 to 0.999), while a decrease occurs with C_2 (which varies from 0.001 to 0.01). A comparison of the theoretical result to the computed one is presented later on (Sect. 4.2).

3.3 Thin cylinder–thick coil

This situation is described by the following relation:

$$R_{\text{cyl}} = \epsilon R_{\text{coil}}, \tag{18}$$

$$C_1 \simeq \epsilon, \tag{19}$$

$$C_2 \simeq 1 - \epsilon. \tag{20}$$

As the coil touches the cylinder here (Fig. 3c), relation (3) becomes

$$R = R_{\text{coil}} + R_{\text{cyl}}. \tag{21}$$

Using relation (18) in Eq. (21) yields

$$R = (1 + \epsilon) R_{\text{coil}} \simeq R_{\text{coil}}. \tag{22}$$

Table 2 Analytical values for non-dimensional coefficient of sensitivity of flowmeter $S_3(C_1, C_2)$ computed as function of non-dimensional parameters C_1 and C_2 (when $C_1 = \epsilon$ and $C_2 = 1 - \epsilon$) and corresponding values for analytical Lorentz force $|F_3|$ (absolute value, unit is N)

C_2	C_1	$S_3(C_1, C_2)$	$\lvert F_3 \rvert$
0.99	0.010	2.58×10^{-7}	1.75×10^{-6}
0.992	0.008	1.32×10^{-7}	8.96×10^{-7}
0.996	0.004	1.65×10^{-8}	1.12×10^{-7}
0.997	0.003	$6{,}96 \times 10^{-9}$	4.75×10^{-8}
0.998	0.002	2.06×10^{-9}	$1{,}41 \times 10^{-8}$
0.999	0.001	2.58×10^{-10}	1.76×10^{-9}

Replacing R_{coil} with R [according to (22)] in Eq. (18) leads to

$$R_{\text{cyl}} = \epsilon R. \tag{23}$$

Equation (23) can be equivalently written as $R_{\text{cyl}} \ll R$ (or $C_1 \ll 1$), which is the condition representing the case investigated in Sect. 3.1. That allows us to adapt Eq. (6) to the situation considered here, replacing R with R_{cyl}/ϵ as

$$F_3 = -\frac{45\pi^2}{256}\frac{\sigma V_0 \mu_0^2 I^2 R_{\text{cyl}} \epsilon^3 S_1}{4},$$

where $S_1 = 1/4$. ϵ is defined from relation (18) as $\epsilon = R_{\text{cyl}}/R_{\text{coil}} = C_1/C_2$. The coefficient of sensitivity of the flowmeter is defined as

$$S_3(C_1, C_2) = S_1 \epsilon^3 = \frac{1}{4}\left(\frac{C_1}{C_2}\right)^3. \tag{24}$$

Henceforth, Eq. (25) is therefore a heuristic formulation to define the Lorentz force created for the thin cylinder–thick coil situation:

$$F_3 = -\frac{45\pi^2}{256}\frac{\sigma V_0 \mu_0^2 I^2 R_{\text{cyl}} S_3(C_1, C_2)}{4}. \tag{25}$$

Table 2 summarizes the coefficient of sensitivity $S_3(C_1, C_2)$ and the Lorentz force calculated analytically for $C_1 = \epsilon$ while $C_2 = 1 - \epsilon$. We clearly observe a decrease of the Lorentz force in the cylinder when C_1 decreases (meaning R_{cyl} becomes tiny).

4 Results of numerical computations

To comprehensively understand the dependence of the sensitivity of the flowmeter on the geometry parameters C_1 and C_2, we performed an extensive set of computations for the axisymmetric problem using commercial software (COMSOL). The height of the translating solid body was taken to be equal to four times the curvature radius of the coil. The radius of the cylinder was fixed at 0.01 m for all computations. The dimensionless number C_2 was fixed to a range of values varying from 0.001 to 0.9, while C_1 was varied by modifying the curvature radius of the coil from 1 m ($C_1 = 0.01$) to a small value close to the radius of the cylinder (up to $C_1 \simeq 0.99$). The numerical results for the coefficient of sensitivity of the flowmeter are used as a function of C_1 and C_2. The computed sensitivity of

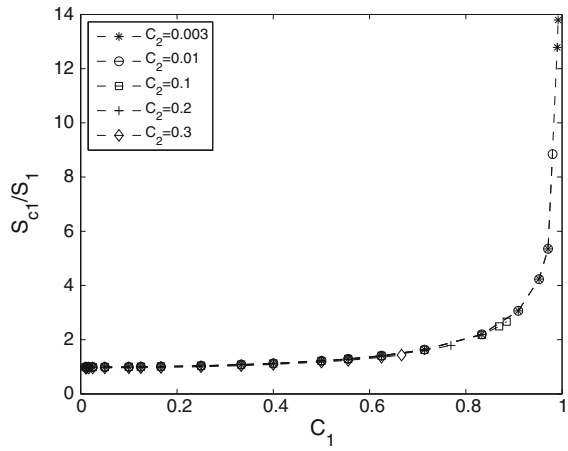

Fig. 5 Ratio of computed to analytical coefficient of sensitivity S_{c1}/S_1 plotted versus C_1 for $C_2 = 0.003$, 0.01, 0.1, 0.2 and 0.3

the flowmeter denoted by S_{c1}, S_{c2} and S_{c3} are respectively deduced from the ratio between the computed Lorentz force and the analytical one, F_c/F_1, F_c/F_2 and F_c/F_3, as

$$\frac{F_c}{F_i} = \frac{S_{ci}}{S_i} \Longrightarrow S_{ci} = \frac{F_c}{F_i} S_i, \tag{26}$$

where $i = 1$, 2 or 3.

The computed Lorentz force is determined by integrating the axial component of the Lorentz force in the solid body domain.

4.1 Sensitivity of flowmeter for thin cylinder–thin coil case: $C_1 = \epsilon$ and $C_2 = \epsilon$

The computed coefficient of sensitivity of the flowmeter, S_{c1}, is obtained from Eq. (26) when the Lorentz force is established for the case where $C_1 = \epsilon$ [with $\epsilon \ll 1$, this condition describes the domain covered by Eq. (5)]. The sensitivity of the flowmeter was analysed as a function of C_1, while C_2 has a fixed value, as shown in Fig. 5. The ratio of the computed to the analytical coefficient of sensitivity S_{c1}/S_1 is plotted versus C_1 for $C_2 = 0.003$, 0.01, 0.1, 0.2 and 0.3. A zoom of Fig. 5 in the region where the ratio S_{c1}/S_1 lies around 1 is presented in Fig. 6a: when C_2 increases, the computed coefficient of sensitivity of the flowmeter becomes smaller than the analytical one. Thus, for $C_2 = 0.3$, for instance, the ratio S_{c1}/S_1 is very close to 0.95, while it is close to 1 when $C_2 = 0.003$. Figure 6b focuses on the values $C_2 = 0.4$, 0.5, 0.6, 0.7, 0.8 and 0.9. Here, the ratio S_{c1}/S_1 moves away from 0.95 (for $C_2 = 0.4$) to 0.7 for $C_2 = 0.9$. This behaviour shows the effect of the non-dimensional parameter C_2 on the coefficient of sensitivity for the case considered here: when C_2 increases and approaches unity, the ratio S_{c1}/S_1 is no longer close to 1 because the condition $C_2 = \epsilon$ is no longer confirmed.

Considering the behaviour along C_1 in Fig. 5, there is good agreement between both the analytical and computed coefficient of sensitivity of the flowmeter up to a range of $C_1 = 0.16$–0.4. The dependency in R_{cyl}^4 of the Lorentz force leads to the curvilinear shape of the graph.

The sensitivity of the flowmeter was also analysed as a function of C_2, with constant C_1 as plotted in Fig. 7. The ratio S_{c1}/S_1 is close to 1 when both C_1 and C_2 have small values. Increasing C_2 induces a decrease in the ratio S_{c1}/S_1, which reaches 0.65 when $C_2 = 0.9$. Similarly, increasing C_1 leads to an increase in the ratio S_{c1}/S_1 up to 2.2 for $C_1 = 0.83$. Note the complementarity of the dimensionless parameters C_1 and C_2: when $C_1 = 0.1$, for instance, the computed data can vary up to 0.9. For higher values of C_1 like 0.83, the data cannot exceed $C_2 = 0.17$.

In summary, the analytical coefficient of sensitivity of the flowmeter is close to the computed one for small values of the dimensionless parameters C_1 and C_2, which agrees with the assumption made in deriving Eq. (5): $C_1 = \epsilon$ and

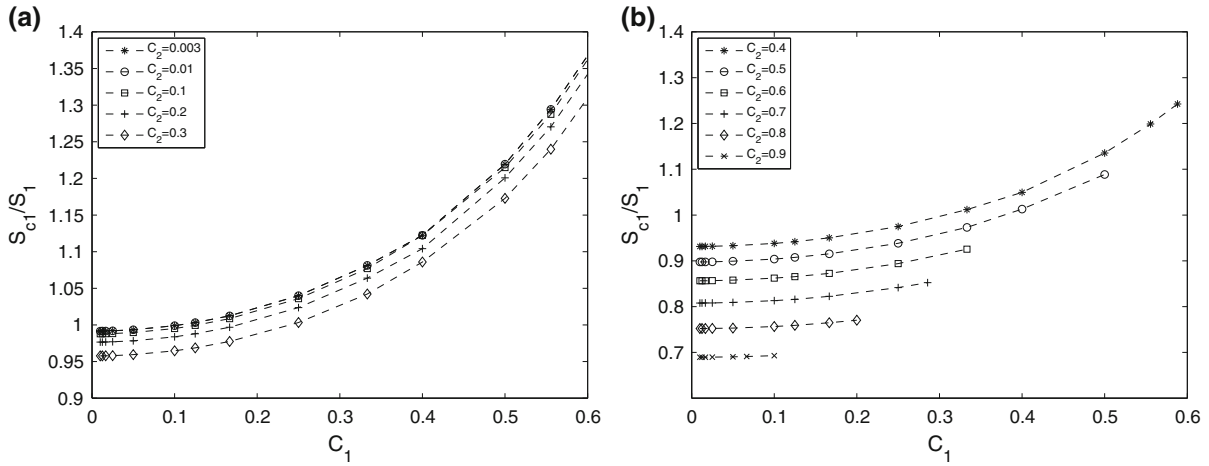

Fig. 6 Ratio of computed to analytical coefficient of sensitivity S_{c1}/S_1. **a** Plotted versus C_1 for $C_2 = 0.003$, 0.01, 0.1, 0.2 and 0.3, focusing on region where S_{c1}/S_1 lies between 0.9 and 1.4. **b** Plotted versus C_1 for $C_2 = 0.4$, 0.5, 0.6, 0.7, 0.8 and 0.9, focusing on region where S_{c1}/S_1 lies between 0.6 and 1.3

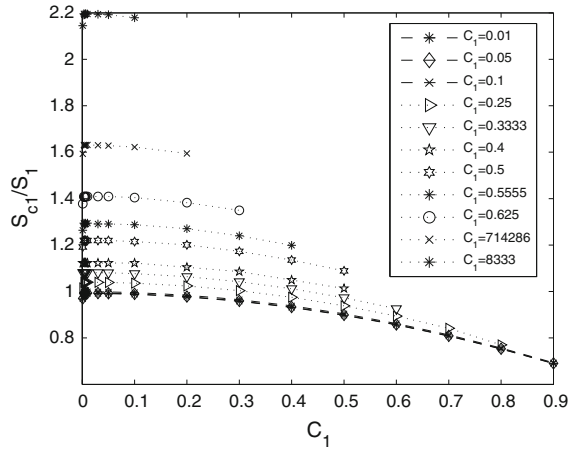

Fig. 7 Ratio of computed to analytical coefficient of sensitivity S_{c1}/S_1 plotted versus C_2 for several values of C_1 from 0.01 to 0.83

$C_2 = \epsilon$. The results presented here serve to validate the computations and enable us to precisely define the domain of validity of the formulated equation: up to $C_1 = 0.16 - 0.4$[2] and $C_2 = 0.007$,[3] Eq. (5) perfectly represents the Lorentz force. Beyond these values, we can consider that the conditions $C_1 = \epsilon$ and $C_2 = \epsilon$ are no longer satisfied.

4.2 Sensitivity of flowmeter for thick cylinder–thin coil case: $C_1 = 1 - \epsilon$ and $C_2 = \epsilon$

As in Sect. 4.1, the coefficient of sensitivity of the flowmeter computed from the ratio F_c/F_2 is analysed here. F_2 is the Lorentz force calculated analytically using Eq. (16). We are interested in the case where $C_1 = 1 - \epsilon$ and $C_2 = \epsilon$, with $\epsilon \ll 1$. The computed coefficient of sensitivity is very close to the analytical one, as shown in Table 3: $S_c/S_2 = 0.989$ when $C_1 = 0.998$ and $C_2 = 0.002$. The values were computed using Eq. (26) for the following parameters: $R = 0.01\,\text{m}$, $C_2 = 1 - C_1$, $\epsilon = C_2/C_1$; R_{cyl} and R_{coil} derive from the known parameters, and C_1 varies between 0.99 and 0.998. The data summarized in Table 3 clearly allow for the conclusion that when the

[2] For these values of C_1, the ratio S_{c1}/S_1 varies between 0.99 and 1.1.

[3] This C_2 value corresponds to a ratio of $S_{c1}/S_1 \simeq 0.99$.

Table 3 Ratio of computed to analytical non-dimensional coefficient of sensitivity of flowmeter S_{c2}/S_2 computed as function of non-dimensional parameters C_1 and C_2 (where dimensionless parameters $C_1 = 1 - \epsilon$ and $C_2 = \epsilon$)

C_1	C_2	S_{c2}/S_2
0.99	0.010	0.680
0.992	0.008	0.717
0.996	0.004	0.860
0.997	0.003	0.924
0.998	0.002	0.989

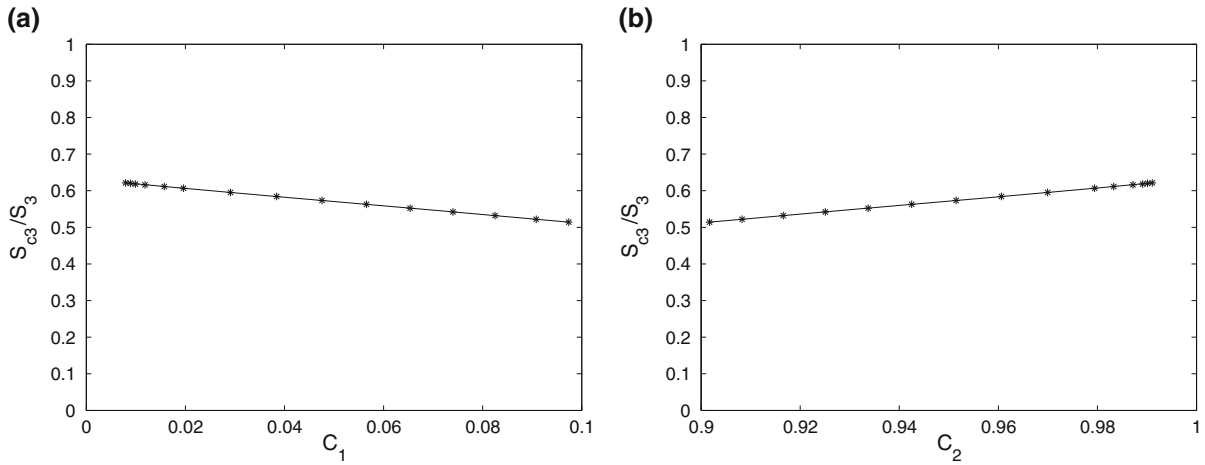

Fig. 8 Ratio of computed to analytical coefficient of sensitivity S_{c3}/S_3 plotted versus C_1 (**a**) and versus C_2 (**b**)

non-dimensional parameters C_1 and C_2 are simultaneously increasing and decreasing respectively, we approach the validity range of Eq. (16). Unlike the case presented in Sect. 4.1, this validity range is quite reduced and the limiting values are $C_1 = 0.997$ and $C_2 = 0.003$.

4.3 Sensitivity of flowmeter for thin cylinder–thick coil case: $C_1 = \epsilon$ and $C_2 = 1 - \epsilon$

This third situation is the opposite of that presented in Sect. 4.2. Here, $C_1 = \epsilon$ and $C_2 = 1 - \epsilon$, with $\epsilon \ll 1$. But, unlike Eq. (16) for the thick cylinder–thin coil case, Eq. (25) was obtained by substitution from Eq. (6) (thin cylinder–thin coil), which leads to a approximate solution for the Lorentz force created in the thin cylinder–thick coil situation. Considering Fig. 8, which presents the ratio S_{c3}/S_3, it can be seen indeed that when $C_1 \to 0.008$ (and $C_2 \to 0.991$), the ratio approaches 0.62, indicating a large gap between the computed and analytical solutions, which is closely linked to the non-accuracy of Eq. (25), even if it behaves well globally. To conclude this last case, we can say that when $C_1 \to \epsilon$ and $C_2 \to 1 - \epsilon$ respectively, we do not have a very accurate, simple formulation with which to efficiently compute the analytical Lorentz force and the coefficient of sensitivity of the flowmeter. Furthermore, it is possible to obtain a semi-analytical solution by applying the Biot–Savart law to the studied geometry to obtain the magnetic field through a complex integration and subsequently deriving the Lorentz force. Such an expression for a magnetic field was established in [14] in the case of a thick rectangular section coil.

4.4 Comparison of three cases

Because it provides the highest value for the Lorentz force, the thick cylinder–thin coil case seems to be best suited for a potential practical application, through some realistic geometrical considerations, such as a gap between the

rod and the electromagnet system. Optimization of the presented arrangements has not been deeply investigated here, but some interesting work in this area is available in the literature, for example in the case of optimizing magnet systems for pipe flows [15].

The power requirement (Joule heating) has been computed for the three arrangements using the following equation:

$$P = RI^2 = \frac{1}{\sigma}\frac{L}{A}I^2, \tag{27}$$

where R (Ohm) is the electrical resistance of the coil, σ (Ohm^{-1} m^{-1}) is its electrical conductivity, L (m) and A (m^2) are the length and the cross section of the coil respectively. Considering $\sigma = 10^7$ Ohm^{-1} m^{-1} it appears that the power dissipated in the case of the thin cylinder–thick coil arrangement is lowest with $P = 201.6$ W (computed for $C_1 = 0.008$ and $C_2 = 0.992$) since thick conductors have less electrical resistance. Accordingly, the thick cylinder–thin coil arrangement presents the highest Joule heating: $P = 2.10^5$ W for $C_1 = 0.99$ and $C_2 = 0.001$ (corresponding to $R_{\text{cyl}} = 0.01$ m and $R_{\text{coil}} = 10^{-5}$ m). An intermediate power of $P = 2000$ W is found for the thin cylinder–thin coil case (for $C_1 = 0.01$ and $C_2 = 0.001$).

Of course, designing such extreme geometries is practically inconceivable, especially the thin coil–thick cylinder case, where a very fine wire coil cannot support so much energy. However, this power calculation aims to show a simple comparison of the three asymptotic cases presented in this paper, knowing that the rank order presented here remains valid when a more realistic situation is appropriately considered for the three situations.

5 Conclusion

A theoretical analysis and numerical modelling of the Lorentz force created inside a solid body which is moving under a steady magnetic field was performed. We determined the equations describing the Lorentz force and the coefficient of sensitivity of the flowmeter as a function of the dimensionless numbers C_1 and C_2 defined for the studied geometry. The computed coefficient of sensitivity of the flowmeter was compared with the derived analytical expression, validating the numerical modelling in the case where the analytical expression was formulated in an earlier study for a thin cylinder–thin coil case, corresponding to regions where $C_1 \ll 1$, regardless of the value reached by C_2. We also showed the validity of computations in the thick cylinder–thin coil situation, in a restrictive region where C_1 tends towards 1 and C_2 tends towards ϵ, with $\epsilon \to 0$. The computation results showed good agreement with the analysis in that region, where the ratio S_{c2}/S_2 (or F_c/F_2) is close to 1. For the last case, thin cylinder–thick coil, only an analytical heuristic formulation was derived for the Lorentz force created inside the moving cylinder. The results presented here show a general behaviour for the coefficient of sensitivity of the flowmeter from asymptotic values of the dimensionless numbers C_1 and C_2, leading to a better understanding of more realistic situations. This outcome produces interesting graphs of the coefficient of sensitivity of the flowmeter according to C_1 and C_2, making it possible to determine quickly the Lorentz force regardless of the geometry considered. The computations also allowed us to define the domain of validity of the thin cylinder–thin coil and the thick cylinder–thin coil cases, which could not be found analytically. Our future full-scale EM–LFV simulations can thus refer to these initial results.

Acknowledgments The authors gratefully acknowledge the financial support of the German Research Foundation (Deutsche Forschungsgemeinschaft) for the Research Training Group (Graduiertenkolleg) Lorentz force velocimetry and Lorentz force eddy current testing and Dr. Thomas Boeck for his helpful criticisms.

References

1. Eckert S, Cramer A, Gerberth G (2007) Velocity measurement techniques for liquid metal flow. Magnetohydrodynamics 80:275–294
2. Shercliff AJ (1962) The theory of electromagnetic flow measurement. Cambridge University Press, Cambridge

3. Feng CC, Deeds WE, Dodd CV (1975) Analysis of eddy-current flowmeters. J Appl Phys 46:2935–2940
4. Priede J, Buchenau D, Gerbeth G (2011) Single-magnet rotary flowmeter for liquid metals. J Appl Phys 110:034512–034520
5. Priede J, Buchenau D, Gerbeth G (2011) Contactless electromagnetic phase-shift flowmeter for liquid metals. Meas Sci Technol 22:055402
6. Thess A, Votyakov E, Kolesnikov Y (2006) Lorentz force velocimetry. Phys Rev Lett 96:164501
7. Thess A, Votyakov E, Knaeppen B, Kolesnikov Y (2007) Theory of the Lorentz force flowmeter. New J Phys 9:299
8. Kirpo M, Tympel S, Boeck T, Krasnov D, Thess A (2011) Electromagnetic drag on a magnetic dipole near a translating conducting bar. J Appl Phys 109:113921
9. Stelian C, Thess A (2011) Optimization of a Lorentz force flowmeter by using numerical modeling. Magnetohydrodynamics 47:273282
10. Kolesnikov Y, Karcher C, Thess A (2011) Lorentz force flowmeter for liquid aluminum: laboratory experiments and plant tests. Metall Mater Trans B 42B:441–450
11. Wang X, Kolesnikov Y, Thess A (2012) Numerical calibration of a Lorentz force flowmeter. Meas Sci Technol 23:045005
12. Wegfrass A, Diethold C, Werner M, Resagk C, Froehlich T, Halbedel B, Thess A (2012) Flow rate measurement of weakly conducting fluids using Lorentz force velocimetry. Meas Sci Technol 23:105307
13. Minchenya V, Karcher C, Kolesnikov Y, Thess A (2011) Calibration of the Lorentz force flowmeter. Flow Meas Instrum 22:242247
14. Babic S, Akyel C (2010) Calculation of the magnetic field created by a thick coil. J Electromagn Waves Appl 24:1405–1418
15. Weidermann C (2013) Design and laboratory test of a Lorentz force flowmeter for pipe flows. PhD Thesis, Fakultaet fuer Maschinenbau der Technischen Universitt Ilmenau